Microwave Devices and Circuits

Third Edition

SAMUEL Y. LIAO

Professor of Electrical Engineering
California State University, Fresno

PRENTICE HALL, *Englewood Cliffs, New Jersey 07632*

Chapter 8

Avalanche Transit-Time Devices

8-0 INTRODUCTION

Avalanche transit-time diode oscillators rely on the effect of voltage breakdown across a reverse-biased *p-n* junction to produce a supply of holes and electrons. Ever since the development of modern semiconductor device theory scientists have speculated on whether it is possible to make a two-terminal negative-resistance device. The tunnel diode was the first such device to be realized in practice. Its operation depends on the properties of a forward-biased *p-n* junction in which both the *p* and *n* regions are heavily doped. The other two devices are the transferred electron devices and the avalanche transit-time devices. In this chapter the latter type is discussed.

The transferred electron devices or the Gunn oscillators operate simply by the application of a dc voltage to a bulk semiconductor. There are no *p-n* junctions in this device. Its frequency is a function of the load and of the natural frequency of the circuit. The avalanche diode oscillator uses carrier impact ionization and drift in the high-field region of a semiconductor junction to produce a negative resistance at microwave frequencies. The device was originally proposed in a theoretical paper by Read [1] in which he analyzed the negative-resistance properties of an idealized n^+-p-i-p^+ diode. Two distinct modes of avalanche oscillator have been observed. One is the IMPATT mode, which stands for *impact ionization avalanche transit-time* operation. In this mode the typical dc-to-RF conversion efficiency is 5 to 10%, and frequencies are as high as 100 GHz with silicon diodes. The other mode is the TRAPATT mode, which represents *trapped plasma avalanche triggered transit* operation. Its typical conversion efficiency is from 20 to 60%.

Another type of active microwave device is the BARITT (*barrier injected transit-time*) diode [2]. It has long drift regions similar to those of IMPATT diodes. The carriers traversing the drift regions of BARITT diodes, however, are generated

by minority carrier injection from forward-biased junctions rather than being extracted from the plasma of an avalanche region. Several different structures have been operated as BARITT diodes, such as *p-n-p*, *p-n-v-p*, *p-n*-metal, and metal-*n*-metal. BARITT diodes have low noise figures of 15 dB, but their bandwidth is relatively narrow with low output power.

8-1 READ DIODE

8-1-1 Physical Description

The basic operating principle of IMPATT diodes can be most easily understood by reference to the first proposed avalanche diode, the Read diode [1]. The theory of this device was presented by Read in 1958, but the first experimental Read diode was reported by Lee et al. in 1965 [3]. A mode of the original Read diode with a doping profile and a dc electric field distribution that exists when a large reverse bias is applied across the diode is shown in Fig. 8-1-1.

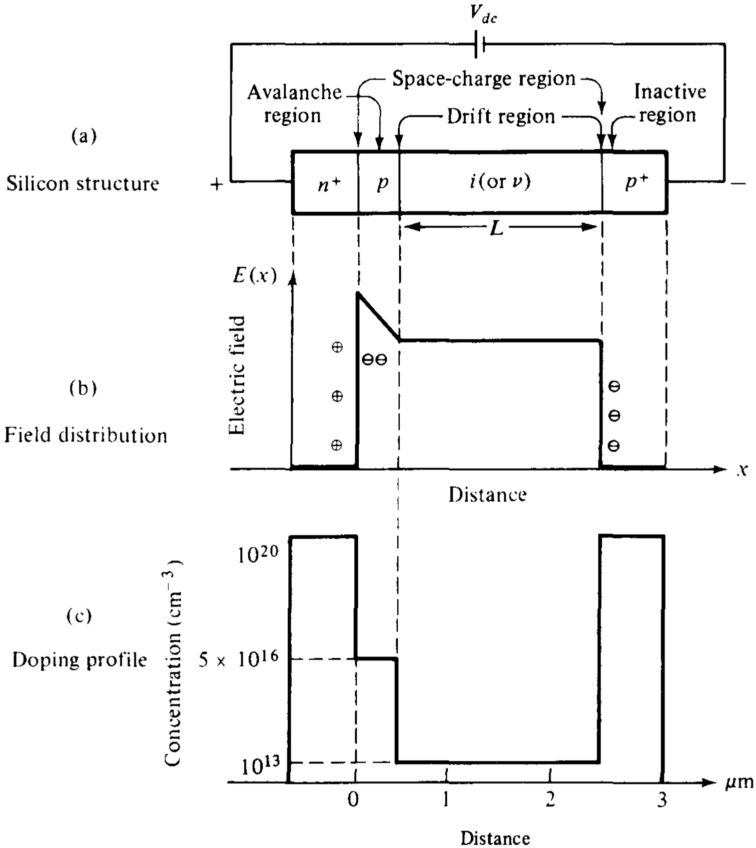

Figure 8-1-1 Read diode.

The Read diode is an n^+-p-i-p^+ structure, where the superscript plus sign denotes very high doping and the i or ν refers to intrinsic material. The device consists essentially of two regions. One is the thin p region at which avalanche multiplication occurs. This region is also called the high-field region or the avalanche region. The other is the i or ν region through which the generated holes must drift in moving to the p^+ contact. This region is also called the intrinsic region or the drift region. The p region is very thin. The space between the n^+-p junction and the i-p^+ junction is called the space-charge region. Similar devices can be built in the p^+-n-i-n^+ structure, in which electrons generated from avalanche multiplication drift through the i region.

The Read diode oscillator consists of an n^+-p-i-p^+ diode biased in reverse and mounted in a microwave cavity. The impedance of the cavity is mainly inductive and is matched to the mainly capacitive impedance of the diode to form a resonant circuit. The device can produce a negative ac resistance that, in turn, delivers power from the dc bias to the oscillation.

8-1-2 Avalanche Multiplication

When the reverse-biased voltage is well above the punchthrough or breakdown voltage, the space-charge region always extends from the n^+-p junction through the p and i regions to the i-p^+ junction. The fixed charges in the various regions are shown in Fig. 8-1-1(b). A positive charge gives a rising field in moving from left to right. The maximum field, which occurs at the n^+-p junction, is about several hundred kilovolts per centimeter. Carriers (holes) moving in the high field near the n^+-p junction acquire energy to knock valence electrons into the conduction band, thus producing hole-electron pairs. The rate of pair production, or avalanche multiplication, is a sensitive nonlinear function of the field. By proper doping, the field can be given a relatively sharp peak so that avalanche multiplication is confined to a very narrow region at the n^+-p junction. The electrons move into the n^+ region and the holes drift through the space-charge region to the p^+ region with a constant velocity v_d of about 10^7 cm/s for silicon. The field throughout the space-charge region is above about 5 kV/cm. The transit time of a hole across the drift i-region L is given by

$$\tau = \frac{L}{v_d} \tag{8-1-1}$$

and the avalanche multiplication factor is

$$M = \frac{1}{1 - (V/V_b)^n} \tag{8-1-1a}$$

where V = applied voltage
V_b = avalanche breakdown voltage
n = 3–6 for silicon is a numerical factor depending on the doping of p^+-n or n^+-p junction

The breakdown voltage for a silicon p^+-n junction can be expressed as

$$|V_b| = \frac{\rho_n \mu_n \epsilon_s |E_{max}|_b^2}{2} \tag{8-1-1b}$$

where ρ_n = resistivity
μ_n = electron mobility
ϵ_s = semiconductor permittivity
E_{max} = maximum breakdown of the electric field

Figure 8-1-2 shows the avalanche breakdown voltage as a function of impurity at a p^+-n junction for several semiconductors.

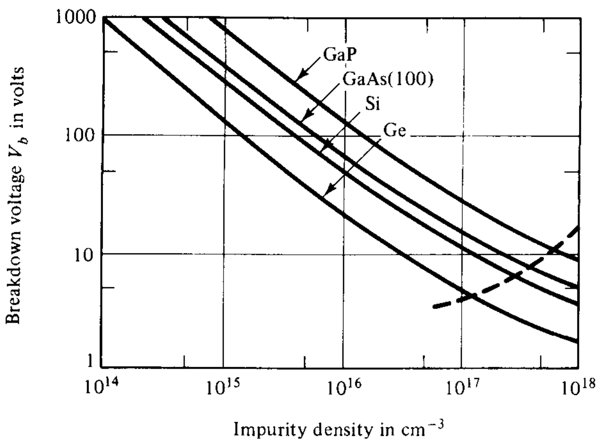

Figure 8-1-2 Breakdown voltage versus impurity doping.

8-1-3 Carrier Current $I_o(t)$ and External Current $I_e(t)$

As described previously, the Read diode is mounted in a microwave resonant circuit. An ac voltage can be maintained at a given frequency in the circuit, and the total field across the diode is the sum of the dc and ac fields. This total field causes breakdown at the n^+-p junction during the positive half of the ac voltage cycle if the field is above the breakdown voltage, and the carrier current (or the hole current in this case) $I_0(t)$ generated at the n^+-p junction by the avalanche multiplication grows exponentially with time while the field is above the critical value. During the negative half cycle, when the field is below the breakdown voltage, the carrier current $I_0(t)$ decays exponentially to a small steady-state value. The carrier current $I_0(t)$ is the current at the junction only and is in the form of a pulse of very short duration as shown in Fig. 8-1-3(d). Therefore the carrier current $I_0(t)$ reaches its maximum in the middle of the ac voltage cycle, or one-quarter of a cycle later than the voltage. Under the influence of the electric field the generated holes are injected into the space-charge region toward the negative terminal. As the injected holes traverse the drift space, they induce a current $I_e(t)$ in the external circuit as shown in Fig. 8-1-3(d).

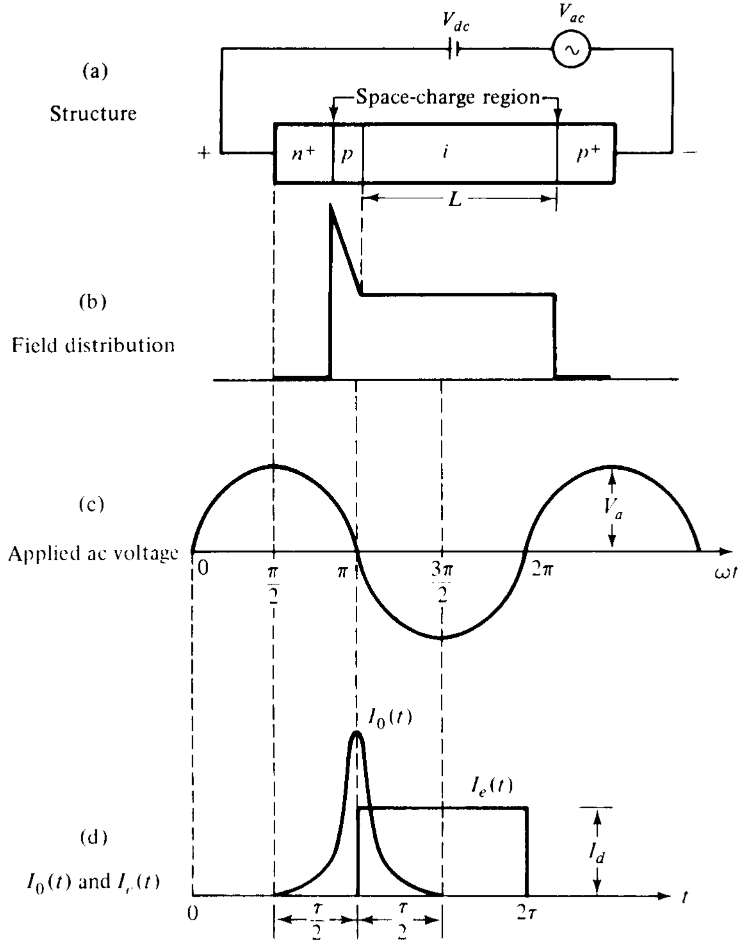

Figure 8-1-3 Field, voltage, and currents in Read diode. (*After Read [1]; reprinted by permission of the Bell System, AT&T Co.*)

When the holes generated at the n^+-p junction drift through the space-charge region, they cause a reduction of the field in accordance with Poisson's equation:

$$\frac{dE}{dx} = -\frac{\rho}{\epsilon_s} \tag{8-1-2}$$

where ρ is the volume charge density and ϵ_s is the semiconductor permittivity.

Since the drift velocity of the holes in the space-charge region is constant, the induced current $I_e(t)$ in the external circuit is simply equal to

$$I_e(t) = \frac{Q}{\tau} = \frac{v_d Q}{L} \tag{8-1-3}$$

where Q = total charge of the moving holes
v_d = hole drift velocity
L = length of the drift i region

It can be seen that the induced current $I_e(t)$ in the external circuit is equal to the average current in the space-charge region. When the pulse of hole current $I_0(t)$ is suddenly generated at the n^+-p junction, a constant current $I_e(t)$ starts flowing in the external circuit and continues to flow during the time τ in which the holes are moving across the space-charge region. Thus, on the average, the external current $I_e(t)$ because of the moving holes is delayed by $\tau/2$ or 90° relative to the pulsed carrier current $I_0(t)$ generated at the n^+-p junction. Since the carrier $I_0(t)$ is delayed by one-quarter of a cycle or 90° relative to the ac voltage, the external current $I_e(t)$ is then delayed by 180° relative to the voltage as shown in Fig. 8-1-3(d). Therefore the cavity should be tuned to give a resonant frequency as

$$2\pi f = \frac{\pi}{\tau}$$

Then

$$f = \frac{1}{2\tau} = \frac{v_d}{2L} \tag{8-1-4}$$

Since the applied ac voltage and the external current $I_e(t)$ are out of phase by 180°, negative conductance occurs and the Read diode can be used for microwave oscillation and amplification. For example, taking $v_d = 10^7$ cm/s for silicon, the optimum operating frequency for a Read diode with an i-region length of 2.5 μm is 20 GHz.

8-1-4 Output Power and Quality Factor Q

The external current $I_e(t)$ approaches a square wave, being very small during the positive half cycle of the ac voltage and almost constant during the negative half cycle. Since the direct current I_d supplied by the dc bias is the average external current or conductive current, it follows that the amplitude of variation of $I_e(t)$ is approximately equal to I_d. If V_a is the amplitude of the ac voltage, the ac power delivered is found to be

$$P = 0.707 V_a I_d \qquad \text{W/unit area} \tag{8-1-5}$$

The quality factor Q of a circuit is defined as

$$Q = \omega \frac{\text{maximum stored energy}}{\text{average dissipated power}} \tag{8-1-6}$$

Since the Read diode supplies ac energy, it has a negative Q in contrast to the positive Q of the cavity. At the stable operating point, the negative Q of the diode is equal to the positive Q of the cavity circuit. If the amplitude of the ac voltage increases, the stored energy, or energy of oscillation, increases faster than the energy

delivered per cycle. This is the condition required in order for stable oscillation to be possible.

8-2 IMPATT DIODES

8-2-1 Physical Structures

A theoretical Read diode made of an n^+-p-i-p^+ or p^+-n-i-n^+ structure has been analyzed. Its basic physical mechanism is the interaction of the impact ionization avalanche and the transit time of charge carriers. Hence the Read-type diodes are called IMPATT diodes. These diodes exhibit a differential negative resistance by two effects:

1. The impact ionization avalanche effect, which causes the carrier current $I_0(t)$ and the ac voltage to be out of phase by 90°
2. The transit-time effect, which further delays the external current $I_e(t)$ relative to the ac voltage by 90°

The first IMPATT operation as reported by Johnston et al. [4] in 1965, however, was obtained from a simple p-n junction. The first real Read-type IMPATT diode was reported by Lee et al. [3], as described previously. From the small-signal theory developed by Gilden [5] it has been confirmed that a negative resistance of the IMPATT diode can be obtained from a junction diode with any doping profile. Many IMPATT diodes consist of a high doping avalanching region followed by a drift region where the field is low enough that the carriers can traverse through it without avalanching. The Read diode is the basic type in the IMPATT diode family. The others are the one-sided abrupt p-n junction, the linearly graded p-n junction (or double-drift region), and the p-i-n diode, all of which are shown in Fig. 8-2-1. The principle of operation of these devices, however, is essentially similar to the mechanism described for the Read diode.

8-2-2 Negative Resistance

Small-signal analysis of a Read diode results in the following expression for the real part of the diode terminal impedance [5]:

$$R = R_s + \frac{2L^2}{v_d \epsilon_s A} \frac{1}{1 - \omega^2/\omega_r^2} \frac{1 - \cos\theta}{\theta} \tag{8-2-1}$$

where R_s = passive resistance of the inactive region
v_d = carrier drift velocity
L = length of the drift space-charge region
A = diode cross section
e_s = semiconductor dielectric permittivity

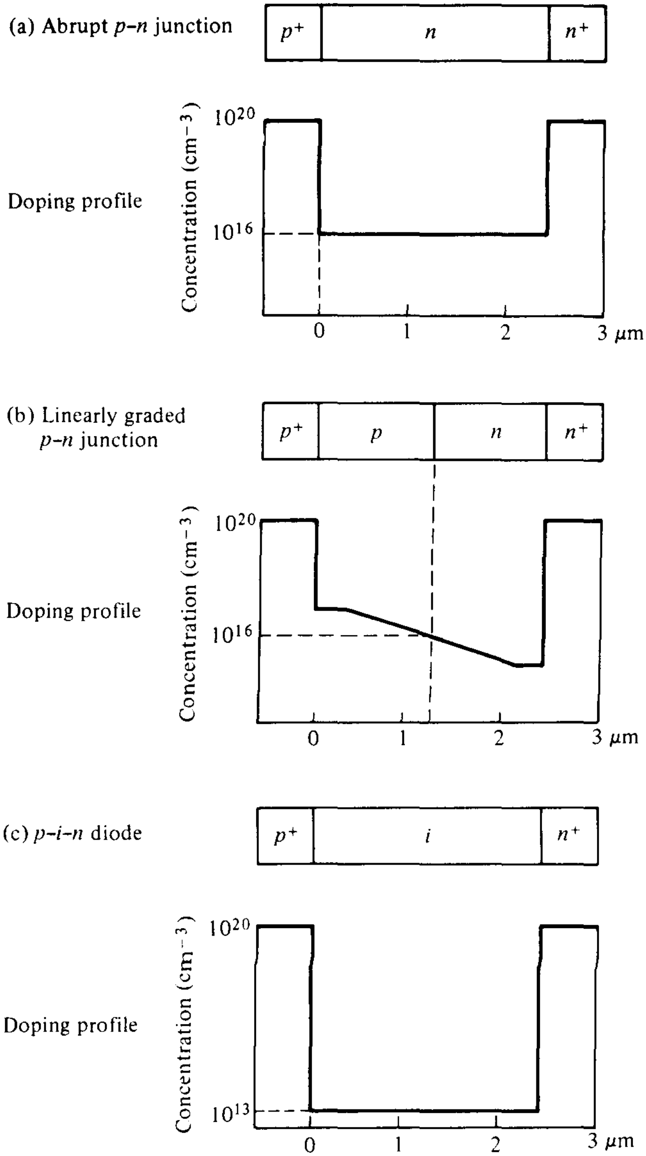

Figure 8-2-1 Three typical silicon IMPATT diodes. (*After R. L. Johnston et al. [4]; reprinted by permission of the Bell System, AT&T Co.*)

Moreover, θ is the transit angle, given by

$$\theta = \omega\tau = \omega\frac{L}{v_d} \tag{8-2-2}$$

and ω_r is the avalanche resonant frequency, defined by

$$\omega_r \equiv \left(\frac{2\alpha' v_d I_0}{\epsilon_s A}\right)^{1/2} \tag{8-2-3}$$

In Eq. (8-2-3) the quantity α' is the derivative of the ionization coefficient with respect to the electric field. This coefficient, the number of ionizations per centimeter produced by a single carrier, is a sharply increasing function of the electric field. The variation of the negative resistance with the transit angle when $\omega > \omega_r$ is plotted in Fig. 8-2-2. The peak value of the negative resistance occurs near $\theta = \pi$. For transit angles larger than π and approaching $3\pi/2$, the negative resistance of the diode decreases rapidly. For practical purposes, the Read-type IMPATT diodes work well only in a frequency range around the π transit angle. That is,

$$f = \frac{1}{2\tau} = \frac{v_d}{2L} \tag{8-2-4}$$

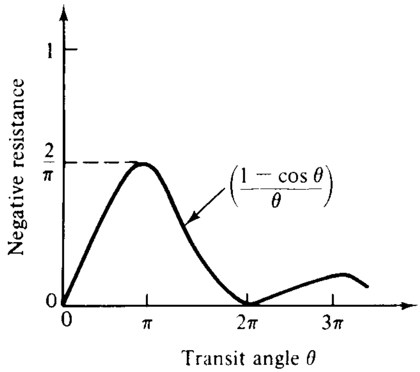

Figure 8-2-2 Negative resistance versus transit angle.

8-2-3 Power Output and Efficiency

At a given frequency the maximum output power of a single diode is limited by semiconductor materials and the attainable impedance levels in microwave circuitry. For a uniform avalanche, the maximum voltage that can be applied across the diode is given by

$$V_m = E_m L \tag{8-2-5}$$

where L is the depletion length and E_m is the maximum electric field. This maximum applied voltage is limited by the breakdown voltage. Furthermore, the maximum current that can be carried by the diode is also limited by the avalanche breakdown process, for the current in the space-charge region causes an increase in the electric field. The maximum current is given by

$$I_m = J_m A = \sigma E_m A = \frac{\epsilon_s}{\tau} E_m A = \frac{v_d \epsilon_s E_m A}{L} \tag{8-2-6}$$

Therefore the upper limit of the power input is given by

$$P_m = I_m V_m = E_m^2 \epsilon_s v_d A \tag{8-2-7}$$

The capacitance across the space-charge region is defined as

$$C = \frac{\epsilon_s A}{L} \tag{8-2-8}$$

Substitution of Eq. (8-2-8) in Eq. (8-2-7) and application of $2\pi f\tau = 1$ yield

$$P_m f^2 = \frac{E_m^2 v_d^2}{4\pi^2 X_c} \tag{8-2-9}$$

It is interesting to note that this equation is identical to Eq. (5-1-60) of the power-frequency limitation for the microwave power transistor. The maximum power that can be given to the mobile carriers decreases as $1/f^2$. For silicon, this electronic limit is dominant at frequencies as high as 100 GHz. The efficiency of the IMPATT diodes is given by

$$\eta = \frac{P_{\text{ac}}}{P_{\text{dc}}} = \left(\frac{V_a}{V_d}\right)\left(\frac{I_a}{I_d}\right) \tag{8-2-10}$$

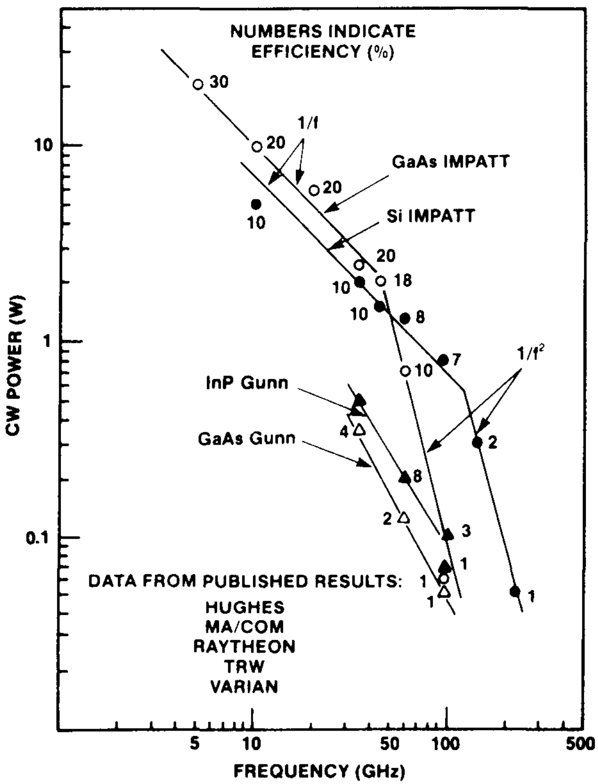

Figure 8-2-3 State-of-the-art performance for GaAs and Si IMPATTs. (*From H. Hieslmair, et al. [6]; reprinted by permission of* Microwave Journal.)

For an ideal Read-type IMPATT diode, the ratio of the ac voltage to the applied voltage is about 0.5 and the ratio of the ac current to the dc current is about $2/\pi$, so that the efficiency would be about $1/\pi$ or more than 30%. For practical IMPATT diodes, however, the efficiency is usually less than 30% because of the space-charge effect, the reverse-saturation-current effect, the high-frequency-skin effect, and the ionization-saturation effect.

IMPATT diodes are at present the most powerful CW solid-state microwave power sources. The diodes have been fabricated from germanium, silicon, and gallium arsenide and can probably be constructed from other semiconductors as well. IMPATT diodes provide potentially reliable, compact, inexpensive, and moderately efficient microwave power sources.

Figure 8-2-3 shows the latest state-of-the-art performance for GaAs and Si IMPATTs [6]. The numbers adjacent to the data points indicate efficiency in percent. Power output data for both the GaAs and Si IMPATTs closely follow the $1/f$ and $1/f^2$ slopes. The transition from the $1/f$ to the $1/f^2$ slope for GaAs falls between 50 and 60 GHz, and that for Si IMPATTs between 100 and 120 GHz. GaAs IMPATTs show higher power and efficiency in the 40- to 60-GHz region whereas Si IMPATTs are produced with higher reliability and yield in the same frequency region. On the contrary, the GaAs IMPATTs have higher powers and efficiencies below 40 GHz than do Si IMPATTs. Above 60 GHz the Si IMPATTs seem to outperform the GaAs devices.

Example 8-2-1: CW Output Power of an IMPATT Diode

An IMPATT diode has the following parameters:

Carrier drift velocity:	$v_d = 2 \times 10^7$ cm/s
Drift-region length:	$L = 6\ \mu$m
Maximum operating voltage:	$V_{0max} = 100$ V
Maximum operating current:	$I_{0max} = 200$ mA
Efficiency:	$\eta = 15\%$
Breakdown voltage:	$V_{bd} = 90$ V

Compute: **(a)** the maximum CW output power in watts; **(b)** the resonant frequency in gigahertz.

Solution

a. From Eq. (8-2-10) the CW output power is

$$P = \eta P_{dc} = 0.15 \times 100 \times 0.2 = 3\text{W}$$

b. From Eq. (8-2-4) the resonant frequency is

$$f = \frac{v_d}{2L} = \frac{2 \times 10^5}{2 \times 6 \times 10^{-6}} = 16.67 \text{ GHz}$$

8-3 TRAPATT DIODES

8-3-1 Physical Structures

The abbreviation TRAPATT stands for *trapped plasma avalanche triggered transit* mode, a mode first reported by Prager et al. [7]. It is a high-efficiency microwave generator capable of operating from several hundred megahertz to several gigahertz. The basic operation of the oscillator is a semiconductor p-n junction diode reverse-biased to current densities well in excess of those encountered in normal avalanche operation. High-peak-power diodes are typically silicon n^+-p-p^+ (or p^+-n-n^+) structures with the n-type depletion region width varying from 2.5 to 12.5 μm. The doping of the depletion region is generally such that the diodes are well "punched through" at breakdown; that is, the dc electric field in the depletion region just prior to breakdown is well above the saturated drift-velocity level. The device's p^+ region is kept as thin as possible at 2.5 to 7.5 μm. The TRAPATT diode's diameter ranges from as small as 50 μm for CW operation to 750 μm at lower frequency for high-peak-power devices.

8-3-2 Principles of Operation

Approximate analytic solutions for the TRAPATT mode in p^+-n-n^+ diodes have been developed by Clorfeine et al. [8] and DeLoach [9] among others. These analyses have shown that a high-field avalanche zone propagates through the diode and fills the depletion layer with a dense plasma of electrons and holes that become trapped in the low-field region behind the zone. A typical voltage waveform for the TRAPATT mode of an avalanche p^+-n-n^+ diode operating with an assumed square-wave current drive is shown in Fig. 8-3-1. At point A the electric field is uniform throughout the sample and its magnitude is large but less than the value required for avalanche breakdown. The current density is expressed by

$$J = \epsilon_s \frac{dE}{dt} \tag{8-3-1}$$

where ϵ_s is the semiconductor dielectric permittivity of the diode.

At the instant of time at point A, the diode current is turned on. Since the only charge carriers present are those caused by the thermal generation, the diode initially charges up like a linear capacitor, driving the magnitude of the electric field above the breakdown voltage. When a sufficient number of carriers is generated, the particle current exceeds the external current and the electric field is depressed throughout the depletion region, causing the voltage to decrease. This portion of the cycle is shown by the curve from point B to point C. During this time interval the electric field is sufficiently large for the avalanche to continue, and a dense plasma of electrons and holes is created. As some of the electrons and holes drift out of the ends of the depletion layer, the field is further depressed and "traps" the remaining plasma. The voltage decreases to point D. A long time is required to remove the plasma because the total plasma charge is large compared to the charge per unit time

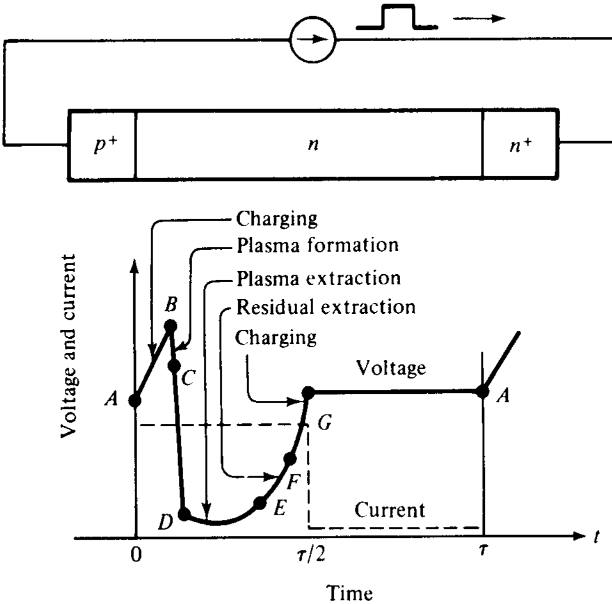

Figure 8-3-1 Voltage and current waveforms for TRAPATT diode. (*After A. S. Clorfeine et al. [8]; reprinted by permission of RCA Laboratory.*)

in the external current. At point E the plasma is removed, but a residual charge of electrons remains in one end of the depletion layer and a residual charge of holes in the other end. As the residual charge is removed, the voltage increases from point E to point F. At point F all the charge that was generated internally has been removed. This charge must be greater than or equal to that supplied by the external current; otherwise the voltage will exceed that at point A. From point F to point G the diode charges up again like a fixed capacitor. At point G the diode current goes to zero for half a period and the voltage remains constant at V_A until the current comes back on and the cycle repeats. The electric field can be expressed as

$$E(x, t) = E_m - \frac{qN_A}{\epsilon_s}x + \frac{Jt}{\epsilon_s} \tag{8-3-2}$$

where N_A is the doping concentration of the n region and x is the distance.

Thus the value of t at which the electric field reaches E_m at a given distance x into the depletion region is obtained by setting $E(x, t) = E_m$, yielding

$$t = \frac{qN_A}{J}x \tag{8-3-3}$$

Differentiation of Eq. (8-3-3) with respect to time t results in

$$v_z \equiv \frac{dx}{dt} = \frac{J}{qN_A} \tag{8-3-4}$$

where v_z is the avalanche-zone velocity.

Example 8-3-1: Avalanche-Zone Velocity of a TRAPATT Diode

A TRAPATT diode has the following parameters:

Doping concentration:	$N_A = 2 \times 10^{15}$ cm^{-3}
Current density:	$J = 20$ kA/cm2

Calculate the avalanche-zone velocity.

Solution From Eq. (8-3-4) the avalanche-zone velocity is

$$v_z = \frac{J}{qN_A} = \frac{20 \times 10^3}{1.6 \times 10^{-19} \times 2 \times 10^{15}} = 6.25 \times 10^7 \text{ cm/s}$$

This means that the avalanche-zone velocity is much larger than the scattering-limited velocity.

Thus the avalanche zone (or avalanche shock front) will quickly sweep across most of the diode, leaving the diode filled by a highly conductng plasma of holes and electrons whose space charge depresses the voltage to low values. Because of the dependence of the drift velocity on the field, the electrons and holes will drift at velocities determined by the low-field mobilities, and the transit time of the carriers can become much longer than

$$\tau_s = \frac{L}{v_s} \tag{8-3-5}$$

where v_s is the saturated carrier drift velocity.

Thus the TRAPATT mode can operate at comparatively low frequencies, since the discharge time of the plasma—that is, the rate Q/I of its charge to its current—can be considerably greater than the nominal transit time τ_s of the diode at high field. Therefore the TRAPATT mode is still a transit-time mode in the real sense that the time delay of carriers in transit (that is, the time between injection and collection) is utilized to obtain a current phase shift favorable for oscillation.

8-3-3 Power Output and Efficiency

RF power is delivered by the diode to an external load when the diode is placed in a proper circuit with a load. The main function of this circuit is to match the diode effective negative resistance to the load at the output frequency while reactively terminating (trapping) frequencies above the oscillation frequency in order to ensure TRAPATT operation. To date, the highest pulse power of 1.2 kW has been obtained at 1.1 GHz (five diodes in series) [10], and the highest efficiency of 75% has been achieved at 0.6 GHz (11). Table 8-3-1 shows the current state of TRAPATT diodes [12].

The TRAPATT operation is a rather complicated means of oscillation, however, and requires good control of both device and circuit properties. In addition,

TABLE 8-3-1 TRAPATT OSCILLATOR CAPABILITIES

Frequency (GHz)	Peak power (W)	Average power (W)	Operating voltage (V)	Efficiency (%)
0.5	600	3	150	40
1.0	200	1	110	30
1.0	400	2	110	35
2.0	100	1	80	25
2.0	200	2	80	30
4.0	100	1	80	20
8.0	50	1	60	15

Source: After W. E. Wilson [12]; reprinted by permission of Horizon House.

the TRAPATT mode generally exhibits a considerably higher noise figure than the IMPATT mode, and the upper operating frequency appears to be practically limited to below the millimeter wave region.

8-4 BARITT DIODES

8-4-1 Physical Description

BARITT diodes, meaning *barrier injected transit-time* diodes, are the latest addition to the family of active microwave diodes. They have long drift regions similar to those of IMPATT diodes. The carriers traversing the drift regions of BARITT diodes, however, are generated by minority carrier injection from forward-biased junctions instead of being extracted from the plasma of an avalanche region.

Several different structures have been operated as BARITT diodes, including *p-n-p*, *p-n-v-p*, *p-n*-metal, and metal-*n*-metal. For a *p-n-v-p* BARITT diode, the forward-biased *p-n* junction emits holes into the ν region. These holes drift with saturation velocity through the ν region and are collected at the *p* contact. The diode exhibits a negative resistance for transit angles between π and 2π. The optimum transit angle is approximately 1.6π.

Such diodes are much less noisy than IMPATT diodes. Noise figures are as low as 15 dB at C-band frequencies with silicon BARITT amplifiers. The major disadvantages of BARITT diodes are relatively narrow bandwidth and power outputs limited to a few milliwatts.

8-4-2 Principles of Operation

A crystal *n*-type silicon wafer with 11 Ω-cm resistivity and 4×10^{14} per cubic centimeter doping is made of a 10-μm thin slice. Then the *n*-type silicon wafer is sandwiched between two PtSi Schottky barrier contacts of about 0.1 μm thickness. A schematic diagram of a metal-*n*-metal structure is shown in Fig. 8-4-1(a).

The energy-band diagram at thermal equilibrium is shown in Fig. 8-4-1(b), where ϕ_{n1} and ϕ_{n2} are the barrier heights for the metal-semiconductor contacts, re-

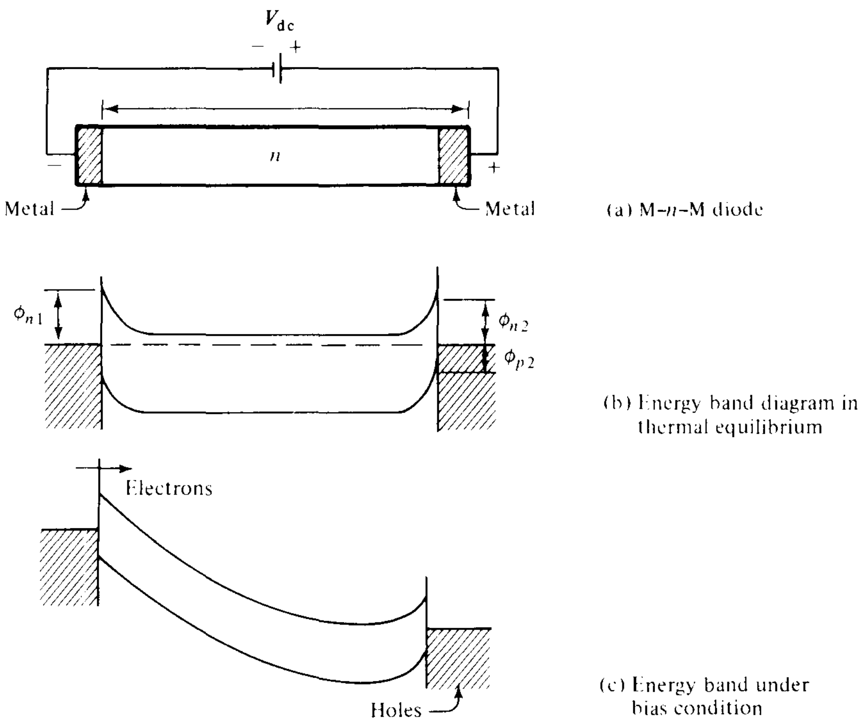

Figure 8-4-1 M-n-M diode. (*After D. J. Coleman and S. M. Sze [13]; reprinted by permission of the Bell System, AT&T Co.*)

spectively. For the PtSi–Si–PtSi structure mentioned previously, $\phi_{n1} = \phi_{n2} = 0.85$ eV. The hole barrier height ϕ_{p2} for the forward-biased contact is about 0.15 eV. Figure 8-4-1(c) shows the energy-band diagram when a voltage is applied. The mechanisms responsible for the microwave oscillations are derived from:

1. The rapid increase of the carrier injection process caused by the decreasing potential barrier of the forward-biased metal-semiconductor contact
2. An apparent $3\pi/2$ transit angle of the injected carrier that traverses the semiconductor depletion region

The rapid increase in terminal current with applied voltage (above 30 V) as shown in Fig. 8-4-2 is caused by thermionic hole injection into the semiconductor as the depletion layer of the reverse-biased contact reaches through the entire device thickness. The critical voltage is approximately given by

$$V_c = \frac{qNL^2}{2\epsilon_s} \tag{8-4-1}$$

where N = doping concentration
L = semiconductor thickness
ϵ_s = semiconductor dielectric permittivity

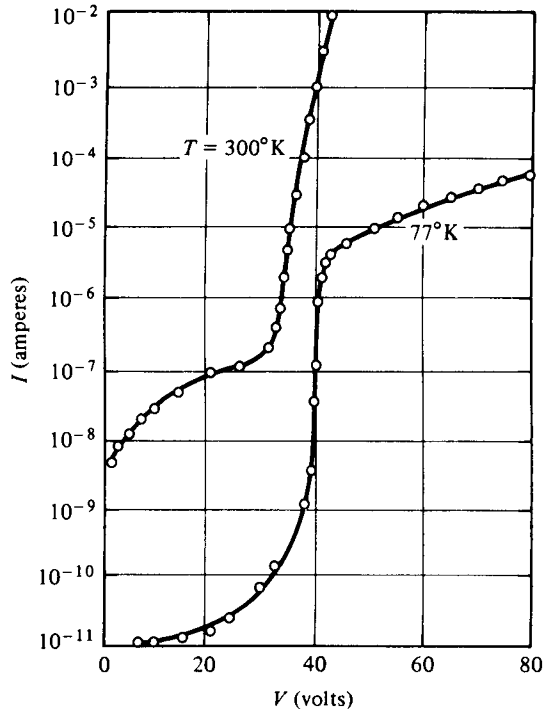

Figure 8-4-2 Current versus voltage of a BARITT diode (PtSi–Si–PtSi). (*After D. J. Coleman and S. M. Sze [13]; reprinted by permission of the Bell System, AT&T Co.*)

The current-voltage characteristics of the silicon MSM structure (PtSi–Si–PtSi) were measured at 77° K and 300° K. The device parameters are $L = 10$ μm, $N = 4 \times 10^{14}$ cm^3, $\phi_{n1} = \phi_{n2} = 0.85$ eV, and area $= 5 \times 10^{-4}$ cm^2.

The current increase is not due to avalanche multiplication, as is apparent from the magnitude of the critical voltage and its negative temperature coefficient. At 77° K the rapid increase is stopped at a current of about 10^{-5} A. This saturated current is expected in accordance with the thermionic emission theory of hole injection from the forward-biased contact with a hole barrier height (ϕ_{p2}) of about 0.15 eV.

8-4-3 Microwave Performance

Continuous-wave (CW) microwave performance of the M-n-M-type BARITT diode was obtained over the entire C band of 4 to 8 GHz. The maximum power observed was 50 mW at 4.9 GHz. The maximum efficiency was about 1.8%. The FM single-sideband noise measure at 1 MHz was found to be 22.8 dB at a 7-mA bias current. This noise measure is substantially lower than that of a silicon IMPATT diode and is comparable to that of a GaAs transfer-electron oscillator. Figure 8-4-3 shows some of the measured microwave power versus current with frequency of operation indicated on each curve for three typical devices tested.

The voltage enclosed in parentheses for each curve indicates the average bias voltage at the diode while the diode is in oscillation. The gain-bandwidth product of a 6-GHz BARITT diode was measured to be 19-dB gain at 5-mA bias current at 200 MHz. The small-signal noise measure was about 15 dB.

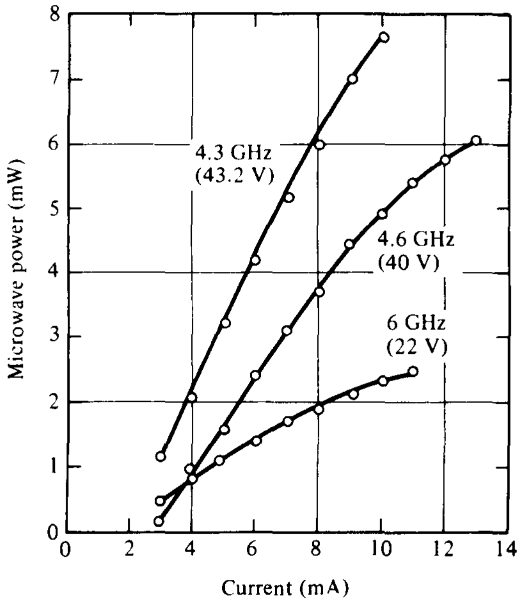

Figure 8-4-3 Power output versus current for three silicon M-n-M devices. (*After D. J. Coleman and S. M. Sze [13]; reprinted by permission of the Bell System, AT&T Co.*)

Example 8-4-1: Breakdown Voltage of a BARITT Diode

An M-Si-M BARITT diode has the following parameters:

Relative dielectric constant of silicon:	$\epsilon_r = 11.8$
Donor concentration:	$N = 2.8 \times 10^{21}\ \mathrm{m}^{-3}$
Silicon length:	$L = 6\ \mu\mathrm{m}$

Determine: **a.** the breakdown voltage; **b.** the breakdown electric field.

Solution

a. From Eq. (8-4-1) the breakdown voltage is double its critical voltage as

$$V_{bd} = \frac{qNL^2}{\epsilon_s} = \frac{1.6 \times 10^{-19} \times 2.8 \times 10^{21} \times (6 \times 10^{-6})^2}{8.854 \times 10^{-12} \times 11.8} = 154.36\ \mathrm{V}$$

b. The breakdown electric field is

$$E_{bd} = \frac{V_{bd}}{L} = \frac{154.36}{6 \times 10^{-6}} = 2.573 \times 10^7\ \mathrm{V/m} = 2.57 \times 10^5\ \mathrm{V/cm}$$

8-5 PARAMETRIC DEVICES

8-5-1 Physical Description

A parametric device is one that uses a nonlinear reactance (capacitance or inductance) or a time-varying reactance. The word *parametric* is derived from the term *parametric excitation,* since the capacitance or inductance, which is a reactive

parameter, can be used to produce capacitive or inductive excitation. Parametric excitation can be subdivided into parametric amplification and oscillation. Many of the essential properties of nonlinear energy-storage systems were described by Faraday [14] as early as 1831 and by Lord Rayleigh [15] in 1883. The first analysis of the nonlinear capacitance was given by van der Ziel [16] in 1948. In his paper van der Ziel first suggested that such a device might be useful as a low-noise amplifier, since it was essentially a reactive device in which no thermal noise is generated. In 1949 Landon [17] analyzed and presented experimental results of such circuits used as amplifiers, converters, and oscillators. In the age of solid-state electronics, microwave electronics engineers dreamed of a solid-state microwave device to replace the noisy electron beam amplifier. In 1957 Suhl [18] proposed a microwave solid-state amplifier that used ferrite. The first realization of a microwave parametric amplifier following Suhl's proposal was made by Weiss [19] in 1957. After the work done by Suhl and Weiss, the parametric amplifier was at last discovered.

At present the solid-state varactor diode is the most widely used parametric amplifier. Unlike microwave tubes, transistors, and lasers, the parametric diode is of a reactive nature and thus generates a very small amount of Johnson noise (thermal noise). One of the distinguishing features of a parametric amplifier is that it utilizes an ac rather than a dc power supply as microwave tubes do. In this respect, the parametric amplifier is analogous to the quantum amplifier laser or maser in which an ac power supply is used.

8-5-2 Nonlinear Reactance and Manley–Rowe Power Relations

A *reactance* is defined as a circuit element that stores and releases electromagnetic energy as opposed to a *resistance,* which dissipates energy. If the stored energy is predominantly in the electric field, the reactance is said to be capacitive; if the stored energy is predominantly in the magnetic field, the reactance is said to be inductive. In microwave engineering it is more convenient to speak in terms of voltages and currents rather than electric and magnetic fields. A capacitive reactance may then be a circuit element for which capacitance is the ratio of charge on the capacitor over voltage across the capacitor. Then

$$C = \frac{Q}{V} \tag{8-5-1}$$

If the ratio is not linear, the capacitive reactance is said to be nonlinear. In this case, it is convenient to define a nonlinear capacitance as the partial derivative of charge with respect to voltage. That is,

$$C(v) = \frac{\partial Q}{\partial v} \tag{8-5-2}$$

The analogous definition of a nonlinear inductance is

$$L(i) = \frac{\partial \Phi}{\partial i} \tag{8-5-3}$$

In the operation of parametric devices, the mixing effects occur when voltages at two or more different frequencies are impressed on a nonlinear reactance.

Small-signal method. It is assumed that the signal voltage v_s is much smaller than the pumping voltage v_p, and the total voltage across the nonlinear capacitance $C(t)$ is given by

$$v = v_s + v_p = V_s \cos(\omega_s t) + V_p \cos(\omega_p t) \tag{8-5-4}$$

where $V_s \ll V_p$. The charge on the capacitor can be expanded in a Taylor series about the point $v_s = 0$, and the first two terms are

$$Q(v) = Q(v_1 + v_p) = Q(v_p) + \left.\frac{dQ(v_p)}{dv}\right|_{v_s=0} v_s \tag{8-5-5}$$

For convenience, it is assumed that

$$C(v_p) = \frac{dQ(v_p)}{dv} = C(t) \tag{8-5-6}$$

where $C(v_p)$ is periodic with a fundamental frequency of ω_p. If the capacitance $C(v_p)$ is expanded in a Fourier series, the result is

$$C(v_p) = \sum_{n=0}^{\infty} C_n \cos(n\omega_p t) \tag{8-5-7}$$

Since v_p is a function of time, the capacitance $C(v_p)$ is also a function of time. Then

$$C(t) = \sum_{n=0}^{\infty} C_n \cos(n\omega_p t) \tag{8-5-8}$$

The coefficients C_n are the magnitude of each harmonic of the time-varying capacitance. In general, the coefficients C_n are not linear functions of the ac pumping voltage v_p. Since the junction capacitance $C(t)$ of a parametric diode is a nonlinear capacitance, the principle of superposition does not hold for arbitrary ac signal amplitudes.

The current through the capacitance $C(t)$ is the derivative of Eq. (8-5-5) with respect to time and it is

$$i = \frac{dQ}{dt} = \frac{dQ(v_p)}{dt} + \frac{d}{dt}[C(t)v_s] \tag{8-5-9}$$

It is evident that the nonlinear capacitance behaves like a time-varying linear capacitance for signals with amplitudes that are much smaller than the amplitude of the pumping voltage. The first term of Eq. (8-5-9) yields a current at the pump frequency f_p and is not related to the signal frequency f_s.

Large-signal method. If the signal voltage is not small compared with the pumping voltage, the Taylor series can be expanded about a dc bias voltage V_0 in a junction diode. In a junction diode the capacitance C is proportional to $(\phi_0 - V)^{-1/2} = V_0^{-1/2}$, where ϕ_0 is the junction barrier potential and V is a negative

voltage supply. Since

$$[V_0 + V_p \cos(\omega_p t)]^{-1/2} \approx V_0^{-1/2}\left(1 - \frac{V_p}{3V_0}\cos(\omega_p t)\right) \qquad \text{for } V_p \ll V_0$$

the capacitance $C(t)$ can be expressed as

$$C(t) = C_0[1 + 2\gamma \cos(\omega_p t)] \tag{8-5-10}$$

The parameter γ is proportional to the pumping voltage v_p and indicates the coupling effect between the voltages at the signal frequency f_s and the output frequency f_0.

Manley–Rowe power relations. Manley and Rowe [20] derived a set of general energy relations regarding power flowing into and out of an ideal nonlinear reactance. These relations are useful in predicting whether power gain is possible in a parametric amplifier. Figure 8-5-1 shows an equivalent circuit for Manley–Rowe derivation.

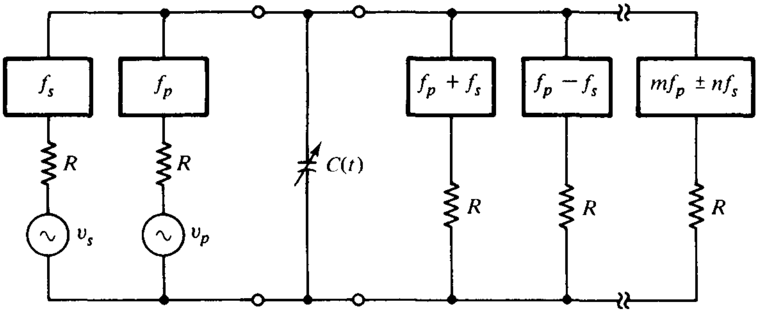

Figure 8-5-1 Equivalent circuit for Manley–Rowe derivation.

In Fig. 8-5-1, one signal generator and one pump generator at their respective frequencies f_s and f_p, together with associated series resistances and bandpass filters, are applied to a nonlinear capacitance $C(t)$. These resonating circuits of filters are designed to reject power at all frequencies other than their respective signal frequencies. In the presence of two applied frequencies f_s and f_p, an infinite number of resonant frequencies of $mf_p \pm nf_p$ are generated, where m and n are any integers from zero to infinity.

Each of the resonating circuits is assumed to be ideal. The power loss by the nonlinear susceptances is negligible. That is, the power entering the nonlinear capacitor at the pump frequency is equal to the power leaving the capacitor at the other frequencies through the nonlinear interaction. Manley and Rowe established the power relations between the input power at the frequencies f_s and f_p and the output power at the other frequencies $mf_p \pm nf_s$.

From Eq. (8-5-4) the voltage across the nonlinear capacitor $C(t)$ can be expressed in exponential form as

$$v = v_p + v_s = \frac{V_p}{2}(e^{j\omega_p t} + e^{-j\omega_p t}) + \frac{V_s}{2}(e^{j\omega_s t} + e^{-j\omega_s t}) \tag{8-5-11}$$

The general expression of the charge Q deposited on the capacitor is given by

$$Q = \sum_{m=-\infty}^{\infty} \sum_{n=-\infty}^{\infty} Q_{m,n} e^{j(m\omega_p t + n\omega_s t)} \tag{8-5-12}$$

In order for the charge Q to be real, it is necessary that

$$Q_{m,n} = Q^*_{-m,-n} \tag{8-5-13}$$

The total voltage v can be expressed as a function of the charge Q. A similar Taylor series expansion of $v(Q)$ shows that

$$v = \sum_{m=-\infty}^{\infty} \sum_{n=-\infty}^{\infty} V_{m,n} e^{j(m\omega_p t + n\omega_s t)} \tag{8-5-14}$$

In order for the voltage v to be real, it is required that

$$V_{m,n} = V^*_{-m,-n} \tag{8-5-15}$$

The current flowing through $C(t)$ is the total derivative of Eq. (8-5-12) with respect to time. This is

$$\begin{aligned} i = \frac{dQ}{dt} &= \sum_{m=-\infty}^{\infty} \sum_{n=-\infty}^{\infty} j(m\omega_p + n\omega_s) Q_{m,n} e^{j(m\omega_p t + n\omega_s t)} \\ &= \sum_{m=-\infty}^{\infty} \sum_{n=-\infty}^{\infty} I_{m,n} e^{j(m\omega_p t + n\omega_s t)} \end{aligned} \tag{8-5-16}$$

where $I_{m,n} = j(m\omega_p + n\omega_s)Q_{m,n}$ and $I_{m,n} = I^*_{-m,-n}$. Since the capacitance $C(t)$ is assumed to be a pure reactance, the average power at the frequencies $mf_p + nf_s$ is

$$\begin{aligned} P_{m,n} &= (V_{m,n} I^*_{m,n} + V^*_{m,n} I_{m,n}) \\ &= (V^*_{-m,-n} I_{-m,-n} + V_{-m,-n} I^*_{-m,-n}) = P_{-m,-n} \end{aligned} \tag{8-5-17}$$

Then conservation of power can be written

$$\sum_{m=-\infty}^{\infty} \sum_{n=-\infty}^{\infty} P_{m,n} = 0 \tag{8-5-18}$$

Multiplication of Eq. (8-5-18) by a factor of $(m\omega_p + n\omega_s)/(m\omega_p + n\omega_s)$ and rearrangement of the resultant into two parts yield

$$\omega_p \sum_{m=-\infty}^{\infty} \sum_{n=-\infty}^{\infty} \frac{mP_{m,n}}{m\omega_p + n\omega_s} + \omega_s \sum_{m=-\infty}^{\infty} \sum_{n=-\infty}^{\infty} \frac{nP_{m,n}}{m\omega_p + n\omega_s} = 0 \tag{8-5-19}$$

Since

$$I_{m,n}/(m\omega_p + n\omega_s) = jQ_{m,n}$$

then $P_{m,n}/(m\omega_p + n\omega_s)$ becomes $-jV_{m,n}Q^*_{m,n} - jV_{-m,-n}Q^*_{-m,-n}$ and is independent of ω_p or ω_s. For any choice of the frequencies f_p and f_s, the resonating circuit external to that of the nonlinear capacitance $C(t)$ can be so adjusted that the currents may keep all the voltage amplitudes $V_{m,n}$ unchanged. The charges $Q_{m,n}$ are then also un-

changed, since they are functions of the voltages $V_{m,n}$. Consequently, the frequencies f_p and f_s can be arbitrarily adjusted in order to require

$$\sum_{m=-\infty}^{\infty} \sum_{n=-\infty}^{\infty} \frac{mP_{m,n}}{m\omega_p + n\omega_s} = 0 \tag{8-5-20}$$

$$\sum_{m=-\infty}^{\infty} \sum_{n=-\infty}^{\infty} \frac{nP_{m,n}}{m\omega_p + n\omega_s} = 0 \tag{8-5-21}$$

Equation (8-5-20) can be expressed as two terms:

$$\sum_{m=0}^{\infty} \sum_{n=-\infty}^{\infty} \frac{mP_{m,n}}{m\omega_p + n\omega_s} + \sum_{m=0}^{\infty} \sum_{n=-\infty}^{\infty} \frac{-mP_{m,n}}{-m\omega_p - n\omega_s} = 0 \tag{8-5-22}$$

Since $P_{m,n} = P_{-m,-n}$, then

$$\sum_{m=0}^{\infty} \sum_{n=-\infty}^{\infty} \frac{mP_{m,n}}{mf_p + nf_s} = 0 \tag{8-5-23}$$

Similarly,

$$\sum_{m=-\infty}^{\infty} \sum_{n=0}^{\infty} \frac{nP_{m,n}}{mf_p + nf_s} = 0 \tag{8-5-24}$$

where ω_p and ω_s have been replaced by f_p and f_s, respectively.

Equations (8-5-23) and (8-5-24) are the standard forms for the Manley–Rowe power relations. The term $P_{m,n}$ indicates the real power flowing into or leaving the nonlinear capacitor at a frequency of $mf_p + nf_s$. The frequency f_p represents the fundamental frequency of the pumping voltage oscillator and the frequency f_s signifies the fundamental frequency of the signal voltage generator. The sign convention for the power term $P_{m,n}$ will follow that power flowing into the nonlinear capacitance or the power coming from the two voltage generators is positive, whereas the power leaving from the nonlinear capacitance or the power flowing into the load resistance is negative.

Consider, for instance, the case where the power output flow is allowed at a frequency of $f_p + f_s$ as shown in Fig. 8-5-1. All other harmonics are open-circuited. Then currents at the three frequencies f_p, f_s, and $f_p + f_s$ are the only ones existing. Under these restrictions m and n vary from -1 through zero to $+1$, respectively. Then Eqs. (8-5-23) and (8-5-24) reduce to

$$\frac{P_{1,0}}{f_p} + \frac{P_{1,1}}{f_p + f_s} = 0 \tag{8-5-25}$$

$$\frac{P_{0,1}}{f_s} + \frac{P_{1,1}}{f_p + f_s} = 0 \tag{8-5-26}$$

where $P_{1,0}$ and $P_{0,1}$ are the power supplied by the two voltage generators at the frequencies f_p and f_s, respectively, and they are considered positive. The power $P_{1,1}$ flowing from the reactance into the resistive load at a frequency of $f_p + f_s$ is considered negative.

The power gain, which is defined as a ratio of the power delivered by the capacitor at a frequency of $f_p + f_s$ to that absorbed by the capacitor at a frequency of f_s as shown in Eq. (8-5-26) is given by

$$\text{Gain} = \frac{f_p + f_s}{f_s} = \frac{f_0}{f_s} \qquad \text{(for modulator)} \tag{8-5-27}$$

where $f_p + f_s = f_o$ and $(f_p + f_s) > f_p > f_s$. The maximum power gain is simply the ratio of the output frequency to the input frequency. This type of parametric device is called the *sum-frequency parametric amplifier* or *up-converter*.

If the signal frequency is the sum of the pump frequency and the output frequency, Eq. (8-5-26) predicts that the parametric device will have a gain of

$$\text{Gain} = \frac{f_s}{f_p + f_s} \qquad \text{(for demodulator)} \tag{8-5-28}$$

where $f_s = f_p + f_o$ and $f_o = f_s - f_p$. This type of parametric device is called the *parametric down-converter* and its power gain is actually a loss.

If the signal frequency is at f_s, the pump frequency at f_p, and the output frequency at f_o, where $f_p = f_s + f_o$, the power $P_{1,1}$ supplied at f_p is positive. Both $P_{1,0}$ and $P_{0,1}$ are negative. In other words, the capacitor delivers power to the signal generator at f_s instead of absorbing it. The power gain may be infinite, which is an unstable condition, and the circuit may be oscillating both at f_s and f_o. This is another type of parametric device, often called a *negative-resistance parametric amplifier*.

8-5-3 Parametric Amplifiers

In a superheterodyne receiver a radio frequency signal may be mixed with a signal from the local oscillator in a nonlinear circuit (the mixer) to generate the sum and difference frequencies. In a parametric amplifier the local oscillator is replaced by a pumping generator such as a reflex klystron and the nonlinear element by a time-varying capacitor such as a varactor diode (or inductor) as shown in Fig. 8-5-2.

In Fig. 8-5-2, the signal frequency f_s and the pump frequency f_p are mixed in the nonlinear capacitor C. Accordingly, a voltage of the fundamental frequencies f_s and f_p as well as the sum and the difference frequencies $mf_p \pm nf_s$ appears across C. If a resistive load is connected across the terminals of the idler circuit, an output voltage can be generated across the load at the output frequency f_o. The output circuit, which does not require external excitation, is called the *idler circuit*. The output (or idler) frequency f_o in the idler circuit is expressed as the sum and the difference frequencies of the signal frequency f_s and the pump frequency f_p. That is,

$$f_o = mf_p \pm nf_s \tag{8-5-29}$$

where m and n are positive integers from zero to infinity.

If $f_o > f_s$, the device is called a parametric *up-converter*. Conversely, if $f_0 < f_s$, the device is known as a parametric *down-converter*.

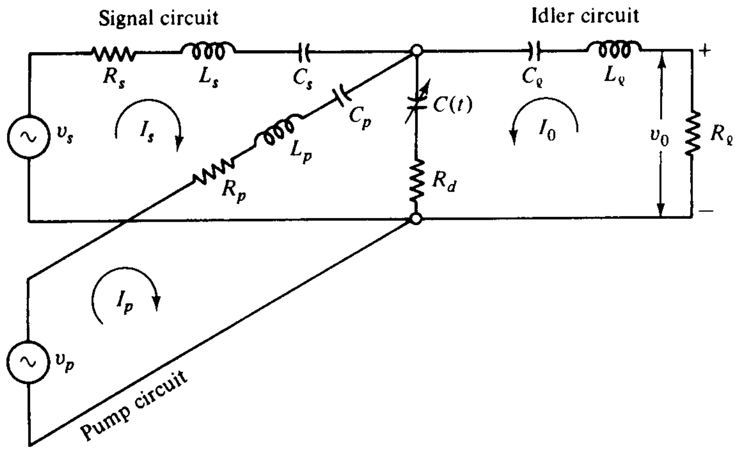

Figure 8-5-2 Equivalent circuit for a parametric amplifier.

Parametric up-converter. A parametric up-converter has the following properties:

1. The ouptut frequency is equal to the sum of the signal frequency and the pump frequency.
2. There is no power flow in the parametric device at frequencies other than the signal, pump, and output frequencies.

Power Gain. When these two conditions are satisfied, the maximum power gain of a parametric up-converter [21] is expressed as

$$\text{Gain} = \frac{f_0}{f_s}\frac{x}{(1+\sqrt{1+x})^2} \tag{8-5-30}$$

where $f_0 = f_p + f_s$

$$x = \frac{f_s}{f_0}(\gamma Q)^2$$

$$Q = \frac{1}{2\pi f_s C R_d}$$

Moreover, R_d is the series resistance of a p-n junction diode and γQ is the figure of merit for the nonlinear capacitor. The quantity of $x/(1+\sqrt{1+x})^2$ may be regarded as a gain-degradation factor. As R_d approaches zero, the figure of merit γQ goes to infinity and the gain-degradation factor becomes equal to unity. As a result, the power gain of a parametric up-converter for a lossless diode is equal to f_o/f_s, which is predicted by the Manley–Rowe relations as shown in Eq. (8-5-27). In a typical microwave diode γQ could be equal to 10. If $f_o/f_s = 15$, the maximum gain given by Eq. (8-5-30) is 7.3 dB.

Noise Figure. One advantage of the parametric amplifier over the transistor amplifier is its low-noise figure because a pure reactance does not contribute thermal noise to the circuit. The noise figure F for a parametric up-converter [21] is given by

$$F = 1 + \frac{2T_d}{T_0}\left[\frac{1}{\gamma Q} + \frac{1}{(\gamma Q)^2}\right] \tag{8-5-31}$$

where T_d = diode temperature in degrees Kelvin
T_0 = 300°K is the ambient temperature in degrees Kelvin
γQ = figure of merit for the nonlinear capacitor

In a typical microwave diode γQ could be equal to 10. If $f_o/f_s = 10$ and T_d = 300°K, the minimum noise figure is 0.90 dB, as calculated by using Eq. (8-5-31).

Bandwidth. The bandwidth of a parametric up-converter is related to the gain-degradation factor of the merit figure and the ratio of the signal frequency to the output frequency. The bandwidth equation [21] is given by

$$BW = 2\gamma\sqrt{\frac{f_o}{f_s}} \tag{8-5-32}$$

If $f_o/f_s = 10$ and $\gamma = 0.2$, the bandwidth (BW) is equal to 1.264.

Example 8-5-1: Up-Converter Parametric Amplifier

An up-converter parametric amplifier has the following parameters:

Ratio of output frequency over signal frequency:	$f_o/f_s = 25$
Figure of merit:	$\gamma Q = 10$
Factor of merit figure:	$\gamma = 0.4$
Diode temperature:	T_d = 350°K

Calculate: (**a**) the power gain in decibels; (**b**) the noise figure in decibels; (**c**) the bandwidth.

Solution

a. From Eq. (8-5-30) the up-converter power gain is

$$\text{Power gain} = \frac{f_o}{f_s}\frac{x}{(1+\sqrt{1+x})^2} = 25 \times \frac{100/25}{(1+\sqrt{1+100/25})^2}$$
$$= 9.55 = 9.80 \text{ dB}$$

b. From Eq. (8-5-31) the noise figure is

$$F = 1 + \frac{2T_d}{T_o}\left[\frac{1}{\gamma Q} + \frac{1}{(\gamma Q)^2}\right] = 1 + \frac{2 \times 350}{300}\left[\frac{1}{10} + \frac{1}{100}\right] = 1.26 = 1 \text{ dB}$$

c. From Eq. (8-5-32) the bandwidth is

$$\text{BW} = 2\gamma\sqrt{\frac{f_o}{f_s}} = 2 \times 0.4 \times (25)^{1/2} = 4$$

Parametric down-converter. If a mode of down conversion for a parametric amplifier is desirable, the signal frequency f_s must be equal to the sum of the pump frequency f_p and the output frequency f_o. This means that the input power must feed into the idler circuit and the output power must move out from the signal circuit as shown in Fig. 8-5-2. The down-conversion gain (actually a loss) is given by [21]

$$\text{Gain} = \frac{f_s}{f_o} \frac{x}{(1 + \sqrt{1 + x})^2} \tag{8-5-33}$$

Negative-resistance parametric amplifier. If a significant portion of power flows only at the signal frequency f_s, the pump frequency f_p, and the idler frequency f_i, a regenerative condition with the possibility of oscillation at both the signal frequency and the idler frequency will occur. The idler frequency is defined as the difference between the pump frequency and the signal frequency, $f_i = f_p - f_s$. When the mode operates below the oscillation threshold, the device behaves as a bilateral negative-resistance parametric amplifier.

Power Gain. The output power is taken from the resistance R_i at a frequency f_i, and the conversion gain from f_s to f_i [21] is given by

$$\text{Gain} = \frac{4f_i}{f_s} \cdot \frac{R_g R_i}{R_{Ts} R_{Ti}} \cdot \frac{a}{(1 - a)^2} \tag{8-5-34}$$

where f_s = signal frequency
f_p = pump frequency
$f_i = f_p - f_s$ is the idler frequency
R_g = output resistance of the signal generator
R_i = output resistance of the idler generator
R_{Ts} = total series resistance at f_s
R_{Ti} = total series resistance at f_i
$a = R/R_{Ts}$
$R = \gamma^2/(\omega_s \omega_i C^2 R_{Ti})$ is the equivalent negative resistance

Noise Figure. The optimum noise figure of a negative-resistance parametric amplifier [21] is expressed as

$$F = 1 + 2\frac{T_d}{T_0}\left[\frac{1}{\gamma Q} + \frac{1}{(\gamma Q)^2}\right] \tag{8-5-35}$$

where γQ = figure of merit for the nonlinear capacitor
T_0 = 300°K is the ambient temperature in degrees Kelvin
T_d = diode temperature in degrees Kelvin

It is interesting to note that the noise figure given by Eq. (8-5-35) is identical to that for the parametric up-converter in Eq. (8-5-31).

Bandwidth. The maximum gain bandwidth of a negative-resistance parametric amplifier [21] is given by

$$\mathrm{BW} = \frac{\gamma}{2}\sqrt{\frac{f_i}{f_s\ \mathrm{gain}}} \tag{8-5-36}$$

If gain = 20 dB, $f_i = 4f_s$, and $\gamma = 0.30$, the maximum possible bandwidth for single-tuned circuits is about 0.03.

Degenerate parametric amplifier. The degenerate parametric amplifer or oscillator is defined as a negative-resistance amplifier with the signal frequency equal to the idler frequency. Since the idler frequency f_i is the difference between the pump frequency f_p and the signal frequency f_s, the signal frequency is just one-half the pump frequency.

Power Gain and Bandwidth. The power gain and bandwidth characteristics of a degenerate parametric amplifier are exactly the same as for the parametric up-converter. With $f_s = f_i$ and $f_p = 2f_s$, the power transferred from pump to signal frequency is equal to the power transferred from pump to idler frequency. At high gain the total power at the signal frequency is almost equal to the total power at the idler frequency. Hence the total power in the passband will have 3 dB more gain.

Noise Figure. The noise figures for a single-sideband and a double-sideband degenerate parametric amplifier [21] are given by, respectively,

$$F_{\mathrm{ssb}} = 2 + \frac{2\overline{T}_d R_d}{T_0 R_g} \tag{8-5-37}$$

$$F_{\mathrm{dsb}} = 1 + \frac{\overline{T}_d R_d}{T_0 R_g} \tag{8-5-38}$$

where $\overline{T}_d$ = average diode temperature in degrees Kelvin
T_0 = 300°K is the ambient noise temperature in degrees Kelvin
R_d = diode series resistance in ohms
R_g = external output resistance of the signal generator in ohms

It can be seen that the noise figure for double-sideband operation is 3 dB less than that for single-sideband operation.

8-5-4 Applications

The choice of which type of parametric amplifier to use depends on the microwave system requirements. The up-converter is a unilateral stable device with a wide bandwidth and low gain. The negative-resistance amplifier is inherently a bilateral and unstable device with narrow bandwidth and high gain. The degenerate parametric amplifier does not require a separate signal and idler circuit coupled by the diode and is the least complex type of parametric amplifier.

In general, the up-converter has the following advantages over the negative-resistance parametric amplifier:

1. A positive input impedance
2. Unconditionally stable and unilateral
3. Power gain independent of changes in its source impedance
4. No circulator required
5. A typical bandwidth on the order of 5%

At higher frequencies where the up-converter is no longer practical, the negative-resistance parametric amplifier operated with a circulator becomes the proper choice. When a low noise figure is required by a system, the degenerate parametric amplifier may be the logical choice, since its double-sideband noise figure is less than the optimum noise figure of the up-converter or the nondegenerate negative-resistance parametric amplifier. Furthermore, the degenerate amplifier is a much simpler device to build and uses a relatively low pump frequency. In radar systems the negative-resistance parametric amplifier may be the better choice, since the frequency required by the system may be higher than the X band. However, since the parametric amplifier is complicated in fabrication and expensive in production, there is a tendency in microwave engineering to replace it with the GaAs metal-semiconductor field-effect transistor (MESFET) amplifier in airborne radar systems.

REFERENCES

[1] READ, W. T., A proposed high-frequency negative-resistance diode. *Bell System Tech. J.*, **37**, 401–446 (1958)

[2] COLEMAN, D. J., JR., and S. M. SZE, A low-noise metal-semiconductor-metal (MSM) microwave oscillator. *Bell System Tech. J.*, **50**, 1695–1699, May–June 1971.

[3] LEE, C. A., ET AL., The Read diode, an avalanche, transit-time, negative-resistance oscillator. *Appl. Phys. Letters*, **6**, 89 (1965).

[4] JOHNSTON, R. L., B. C. DELOACH, and G. B. COHEN, A silicon diode microwave oscillator. *Bell System Tech. J.*, **44**, 369–372, February 1965.

[5] GILDEN, M., and M. E. HINES, Electronic tuning effects in the Read microwave avalanche diode. *IEEE Trans. on Electron Devices*, **ED-13**, 5–12, January 1966.

[6] HIESLMAIR, H., ET AL., State of the art of solid-state and tube transmitters. *Microwave J.*, **26**, No. 10, 46–48, October 1983.

[7] PRAGER, H. J., ET AL., High-power, high-efficiency silicon avalanche diodes at ultra high frequencies. *Proc. IEEE* (*Letters*), **55**, 586–587, April 1967.

[8] CLORFEINE, A. S., ET AL., A theory for the high-efficiency mode of oscillation in avalanche diodes. *RCA Rev.*, **30**, 397–421, September 1969.

[9] DELOACH, B. C., JR., and D. L. SCHARFETTER, Device physics of TRAPATT oscillators. *IEEE Trans. on Electron Devices*, **ED-17**, 9–21, January 1970.

[10] LIU, S. G., and J. J. RISKA, Fabrication and performance of kilowatt L-band avalanche diodes. *RCA Rev.*, **31,** 3, March 1970.

[11] KOSTICHACK, D. F., UHF avalanche diode oscillator providing 400 watts peak power and 75 percent efficiency. *Proc. IEEE (Letters),* **58,** 1282–1283, August 1970.

[12] WILSON, W. E., Pulsed LSA and TRAPATT sources for microwave systems. *Microwave J.,* **14,** No. 8, 33–41, August 1971.

[13] COLEMAN, D. J., JR., and S. M. SZE, A low-noise metal-semiconductor-metal (MSM) microwave oscillator. *Bell System Tech. J.,* 1675–1695, May–June 1971.

[14] FARADAY, M., On a peculiar class of acoustical figures; and certain forms assumed by a group of particles upon vibrating elastic surface. *Phil. Trans. Roy. Soc. (London),* **121,** 299–318, May 1831.

[15] LORD RAYLEIGH, and J. W. STRUTT, On the crispations of fluid resting upon a vibrating support. *Phil. Mag.,* **16,** 50–53, July 1883.

[16] VAN DER ZIEL, A., On the mixing properties of nonlinear capacitances. *J. Appl. Phys.,* **19,** 999–1006, November 1948.

[17] LANDON, V. D., The use of ferrite cored coils as converters, amplifiers, and oscillators. *RCA Rev.,* **10,** 387–396, September 1949.

[18] SUHL, H., Proposal for a ferromagnetic amplifier in the microwave range. *Phys. Rev.,* **106,** 384–385, April 15, 1957.

[19] WEISS, M. T., A solid-state microwave amplifier and oscillator using ferrites. *Phys Rev.,* **107,** 317, July 1957.

[20] MANLEY, J. M., and H. E. ROWE, Some general properties of nonlinear elements—Pt. I, General energy relations. *Proc. IRE,* **44,** 904–913, July 1956.

[21] BLACKWELL, L. A., and K. L. KOTZEBUE, *Semiconductor-Diode Parametric Amplifiers,* 41, 42, 45, 53, 57, 62, 70. Prentice-Hall, Inc., Englewood Cliffs, N.J., 1961.

SUGGESTED READINGS

CHANG, K. K. N., *Parametric and Tunnel Diodes.* Prentice-Hall, Inc., Englewood Cliffs, N.J., 1964.

DELOACH, B. C., and D. L. SCHARFETTER, Device physics of TRAPATT oscillators. *IEEE Trans. on Electron Devices,* **ED-17,** No. 1, 9–21, January 1970.

EASTMAN, L. F., *Gallium Arsenide Microwave Bulk and Transit-Time Devices.* Artech House, Dedham, Mass., 1973.

HADDAD, G. I., ed., *Avalanche Transit-Time Devices.* Artech House, Dedham, Mass., 1973.

HADDAD, G. I., ET AL., Basic principles and properties of avalanche transit-time devices. *IEEE Trans. on Microwave Theory and Techniques,* **MTT-18,** No. 11, 752–772, November 1970.

MILNES, A. G., *Semiconductor Devices and Integrated Electronics.* Van Nostrand Reinhold Company, New York, 1980.

PARKER, D., TRAPATT oscillations in a *p-i-n* avalanche diode. *IEEE Trans. on Electron Devices,* **ED-18,** No. 5, 281–293, May 1971.

SZE, S. M., Microwave avalanche diodes. *IEEE Proc.,* **59,** No.8, 1140–1171, August 1971.

PROBLEMS

Avalanche Transit-Time Devices

8-1. Spell out the following abbreviated terms: IMPATT, TRAPATT, and BARITT.

8-2. Derive Eq. (8-2-9).

8-3. Describe the operating principles of the Read diode, IMPATT diode, TRAPATT diode, and BARITT diode.

8-4. An IMPATT diode has a drift length of 2 μm. Determine: (**a**) the drift time of the carriers and (**b**) the operating frequency of the IMPATT diode.

8-5. A Ku-band IMPATT diode has a pulsed-operating voltage of 100 V and a pulsed-operating current of 0.9 A. The efficiency is about 10%. Calculate:
a. The output power
b. The duty cycle if the pulse width is 0.01 ns and the frequency is 16 GHz

8-6. An M-Si-M BARITT diode has the following parameters:

Relative dielectric constant of Si:	$\epsilon_r = 11.8$
Donor concentration:	$N = 3 \times 10^{21}$ m^{-3}
Si length:	$L = 6.2$ μm

Calculate: (**a**) the breakdown voltage and (**b**) the breakdown electric field.

Parametric Devices

8-7. **a.** Describe the advantages and disadvantages of the parametric devices.
b. Describe the applications of the parametric amplifiers.

8-8. The figure of merit for a diode nonlinear capacitor in an up-converter parametric amplifier is 8, and the ratio of the output (or idler) frequency f_o over the signal frequency f_s is 8. The diode temperature is 300°K.
a. Calculate the maximum power gain in decibels.
b. Compute the noise figure F in decibels.
c. Determine the bandwidth (BW) for $\gamma = 0.2$.

8-9. A negative-resistance parametric amplifier has the following parameters:

$f_s = 2$ GHz	$R_i = 1$ kΩ	$\gamma = 0.35$
$f_p = 12$ GHz	$R_g = 1$ KΩ	$\gamma Q = 10$
$f_i = 10$ GHz	$R_{Ts} = 1$ KΩ	$T_d = 300°$K
$f_i = 5f_s$	$R_{Ti} = 1$ KΩ	$C = 0.01$ pF

a. Calculate the power gain in decibels.
b. Compute the noise figure F in decibels.
c. Determine the bandwidth (BW).